Bull. Korean Chem. Soc. 2014, Vol. 35, No. 5 1279
http://dx.doi.org/10.5012/bkcs.2014.35.5.1279

Articles

Label-free Detection of the Transcription Initiation Factor Assembly and Specific Inhibition by Aptamers

Shuo Ren,[a] Yuanyuan Jiang,[a] Hye Rim Yoon, Sun Woo Hong,[†] Donghyuk Shin,[‡] Sangho Lee,[‡] Dong-ki Lee,[†] Moonsoo M. Jin,[§] Irene M. Min, and Soyoun Kim[*]

Department of Biomedical Engineering, Dongguk University, Seoul 100-715, Korea. [*]Email: Skim@dongguk.edu
[†]Global Research Laboratory for RNAi Medicine, Department of Chemistry, Sungkyunkwan University, Suwon 440-746, Korea
[‡]Department of Biological Sciences, Sungkyunkwan University, Suwon 440-746, Korea
[§]Department of Radiology, Weill Cornell Medical College, New York, NY 10065, USA
Received December 20, 2013, Accepted December 30, 2013

The binding of TATA-binding protein (TBP) to the TATA-box containing promoter region is aided by many other transcriptional factors including TFIIA and TFIIB. The mechanistic insight into the assembly of RNA polymerase II preinitation complex (PIC) has been gained by either directly altering a function of target protein or perturbing molecular interactions using drugs, RNAi, or aptamers. Aptamers have been found particularly useful for studying a role of a subset of PIC on transcription for their ability to inhibit specific molecular interactions. One major hurdle to the wide use of aptamers as specific inhibitors arises from the difficulty with traditional assays to validate and determine specificity, affinity, and binding epitopes for aptamers against targets. Here, using a technique called the bio-layer interferometry (BLI) designed for a label-free, real-time, and multiplexed detection of molecular interactions, we studied the assembly of a subset of PIC, TBP binding to TATA DNA, and two distinct classes of aptamers against TPB in regard to their ability to inhibit TBP binding to TFIIA or TATA DNA. Using BLI, we measured not only equilibrium binding constants (K_D), which were overall in close agreement with those obtained by electrophoretic mobility shift assay, but also kinetic constants of binding (k_{on} and k_{off}), differentiating aptamers of comparable K_Ds by their difference in binding kinetics. The assay developed in this study can readily be adopted for high throughput validation of candidate aptamers for specificity, affinity, and epitopes, providing both equilibrium and kinetic information for aptamer interaction with targets.

Key Words : SELEX, Aptamer, Transcription factor, BLI

Introduction

Transcription initiation requires the assembly of the pre-initiation complex at the promoter. TBP belongs to a class of general transcriptional factors and binds to a specific DNA sequence called the TATA box, which is found in the promoter region of genes in archaea and eukaryotes.[1] TBP binding to TATA box needs to be further stabilized by other general transcriptional factors including TFIIA and TFIIB in order for RNA polymerase to initiate transcription. The roles of transcriptional factors and nucleic acids, and their interaction in transcription have been elucidated primarily by structural studies and the use of mutants. Alternative to directly altering inherent properties of transcriptional factors by mutations, RNA aptamers have emerged as a useful tool to perturb target interactions in a dynamic and reversible manner.[2,3]

Aptamers are single oligonucleotides of 20-100 bp in length, which bind target molecules ranging from small molecules and peptides to large proteins with high affinity and specificity. Aptamers against a variety of transcriptional factors, *e.g.*, TBP, TFIIB, HSF, NF-κB, *etc.*, have been generated and used to probe the effect of specific interactions on transcription.[4-7] Selection of aptamers, called systematic evolution of ligands by exponential enrichment (SELEX), requires typically ~10 rounds of SELEX until desired affinity is obtained.[8,9] The advent of the high throughput sequencing technology now enables a selection of candidate aptamers using shorter rounds of SELEX by sequence analysis, relying on the assumption that specific aptamers are more likely to be the sequences that appear more frequently and become enriched with increasing rounds.[10,11] Even after the candidate aptamers have been identified, with conventional methods the task still remains a challenge for final validation of candidate aptamers including measuring binding affinity and specificity, and mapping aptamer epitopes. Frequently used assays such as electrophoretic mobility shift assay (EMSA), filter binding, and UV crosslinking are tedious and time-

[a]These authors contributed equally to this work.

consuming, and are largely incompatible with a high throughput discovery of aptamers.[12-14]

Compared with the assays requiring labeling of aptamers or targets by fluorescence or luminescence tags, or radioisotopes, the label-free methods provide a real-time monitoring of molecular interactions, extending analysis to both equilibrium and kinetic properties. Similar to the working principles behind the widely used technique called surface plasmon resonance, the bio-layer interferometry (BLI) measures biomolecular interactions by a change in the optical thickness (which is detected as a wavelength shift in the interference pattern) at the biosensor tip caused by the binding of soluble analytes to targets immobilized to the tip surface of the biosensor.[15] In this study, we developed an assay using BLI to measure RNA aptamer interactions with DNA and target proteins in a real-time, multiplexed manner. The affinity of aptamers to targets was determined by BLI using steady-state or kinetic analyses. Furthermore, we also showed the assembly of transcription preinitiation complex involving DNA, TBP, and TFIIA in real-time and its specific inhibition by TBP aptamers.

Experimental

Protein Preparation. Yeast TBP and TFIIA proteins were expressed and purified following the methods described previously.[16] Briefly, his-tagged full-length TBP was expressed from *BL21-DE3* bacteria (NEB, USA) and purified using Ni-NTA affinity resin (Qiagen, Germany), followed by Hi-trap heparin column (GE Healthcare, USA). Yeast TFIIA, consisting of two subunits (TFIIAαβ and TFIIAγ), was expressed in *BL21-DE3* cells, and the cell lysates were suspended in 8 M urea and dialyzed against refolding buffer (30 mM Tris-HCl, pH 8.0, 2 mM EDTA, 10% glycerol, and 500 mM KCl). TFIIA was further purified by ion exchange chromatography using a mono Q column connected to AKTA system (GE Healthcare, USA). Both TBP and TFIIA were confirmed to be more than 95% pure by SDS-PAGE. Protein concentration was measured by Bradford assay, and purified proteins were stored at −70 ºC prior to use.

Synthesis of RNA Aptamers. RNA aptamer candidates were prepared by *in vitro* transcription (MEGAshortscript kit, Ambion, Life technologies, USA) following the manufacturer's protocol. The mixture of RNA and DNA template was treated by DNase for 20 min at 37 ºC, and RNA aptamers were further purified by denaturing polyacrylamide–urea gel electrophoresis. The RNA band was excised from gel and eluted into gel elution buffer (500 mM Ammonium acetate, 1 mM EDTA pH 8.0, 0.1% SDS). Eluted RNA was further purified by phenol-chloroform extraction and ethanol precipitation. Later, RNA pellet was resuspended in DEPC-treated water and the concentration of RNA was measured by absorbance (NanoDrop, 2000 Thermo scientific, USA).

Biotinylation of RNA Aptamers. RNA aptamers were biotinylated at the 3' end by T4 RNA ligase, performed with RNA 3'-end biotinylation kit (Pierce, Thermo scientific, USA). In a typical 30 μL reaction, about 50 pmol of purified RNA was mixed with a 20-fold molar excess of biotinylated cytidine bisphosphate in reaction buffer (40 U T4 RNA ligase, 40 U RNase Inhibitor, 25% DMSO in 0.5 M Tris-HCl pH 7.8, 0.1 M $MgCl_2$, 0.1 M DTT, 10 mM ATP). After incubation of this mixture at 16 °C overnight, unincorporated biotinylated cytidine bisphosphates were removed from RNA aptamers using a desalting column, and biotinylated RNA was further purified by phenol-chloroform extraction and ethanol precipitation. Purified RNA was resuspended in DEPC-treated water and stored at −20 ºC prior to use.

Preparation of TATA-DNA. TATA-DNA was synthesized following the sequence of 5'-biotin-GGGAATTCGGGCTA TAAAAGGGGGATCCGG-3', which was annealed to its complementary strand (IDT, USA) in 1x binding buffer (12 mM HEPES pH 7.9, 100 mM NaCl, 10 mM $MgCl_2$, 1 mM DTT) at 75 ºC for 5 min and cooled to RT.[3]

Real-time, Label-free Measurements of Aptamer and Target Interactions by BLI. ForteBio Octet RED 384™ and streptavidin-coated (SA) sensors (Pall life sciences, USA) were used to study interactions between aptamer candidates and TBP protein, and the assembly and inhibition by aptamers of transcription pre-initiation complex. Unless specified otherwise, assay buffer (1x binding buffer containing 0.1% BSA and 0.02% Tween20) was used for BLI. SA sensors (Cat: 18-5019, Pall life sciences, USA) were prewetted in assay buffer for 30 min prior to incubation with different molecules for 20 min at 25 ºC. The sensors were subject to shaking (1,000 rpm) to promote specific interaction and to reduce non-specific binding. Sensors were dipped into individual wells in 384-microwell plates (100 μL/well) containing TATA-DNA (200 nM) or aptamers (200 nM). To monitor non-specific binding to biosensor, a reference sensor (without loading of biotinylated aptamers or TATA-DNA) was included and subjected to the same procedure as the sensors loaded with biotinylated nucleic acids. Kinetic constants (k_{on} (association constant; $M^{-1}s^{-1}$), k_{off} (dissociation constant; s^{-1})) were approximated by fitting the reaction model for 1:1 kinetics to the reference-subtracted data. The equilibrium dissociation constant (K_D) was computed as a ratio of k_{off} to k_{on}. The Langmuir adsorption equation was fit to the steady-state response to estimate equilibrium dissociation constants.[17]

Results and Discussion

Real-time, Multiplexed Detection of Aptamer Binding to TBP by BLI. The binding of analytes in solution to the biosensor increases the thickness of biological layer on the tip surface, which is then detected by BLI as an interference wavelength shift.[18] To measure the binding of multiple TBP aptamers in parallel (the list of aptamers is shown in Supplementary Table 1), biotinylated aptamers were attached to the SA sensors (phase 'I' in Fig. 1(a)). The sensors were then transferred to the wells filled with assay buffer (phase 'II') and then to the wells containing TPB in assay buffer to record the kinetics of TBP interaction with aptamers (phase 'III'). The dissociation of TBP from aptamers was then

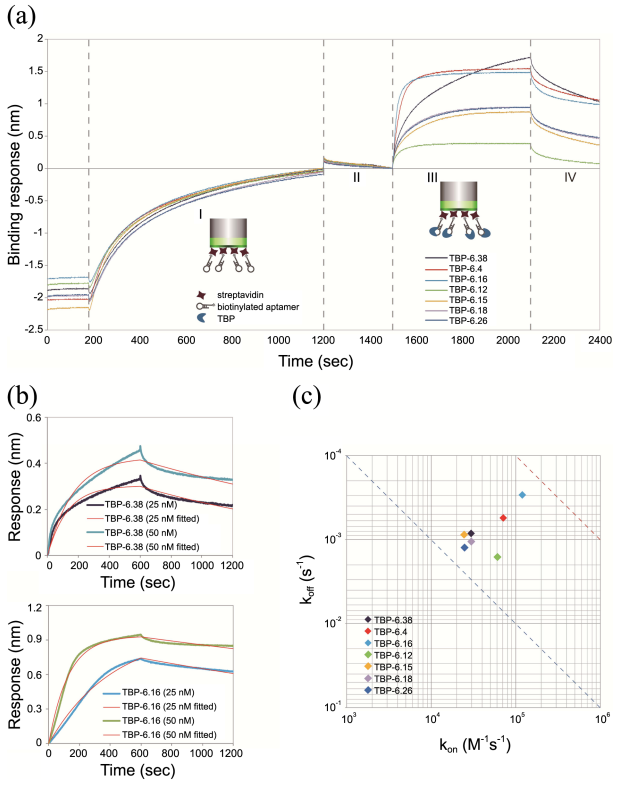

Figure 1. Real-time, multiplexed measurements and analysis of TBP interaction with aptamers using BLI. (a) Using the BLI technique, a real-time assay was developed to rapidly and simultaneously screen aptamer binding to targets. First, SA sensors were loaded with a biotinylated-aptamer (labeled with 'I') and washed to remove non-specific binding ('II'). Subsequently, sensors were incubated in wells containing 500 nM of TBP protein ('III') and then incubated in assay buffer ('IV') to measure association and dissociation kinetics, respectively. (b) The 1:1 rate equation was fitted simultaneously and globally to association and dissociation phase data (the kinetics of binding of TBP-6.38 and TBP-6.16 to TBP are shown as representative examples) to compute the kinetic constants (k_{on} and k_{off}). (c) The kinetic constants of binding for selected aptamers are plotted. Blue and red dashed lines mark the equilibrium dissociation constants (K_D) at 100 and 1 nM, respectively.

measured when the sensors were placed into the wells without TBP in assay buffer (phase 'IV'). Control sensor, which was included to record reference readouts, was prepared without biotinylated aptamers on the tip surface, but was treated in the same way as the aptamer-coated sensors. Real-time measurements of TBP interaction with different aptamers by BLI were then used to compute the equilibrium dissociation (K_D) and kinetic rate constants (k_{on} and k_{off}) by fitting the rate equation for 1:1 kinetics to the data (Fig. 1(b) & (c)). The dissociation constants for aptamer binding to TBP measured by BLI were close to those obtained by EMSA (for TBP-101 and TBP-12; Supplementary Table 1) and by a sol-gel technique (for TBP-6.16). Larger discrepancy was observed for the aptamers isolated mainly by sol-gel SELEX and whose affinity to TBP was also measured by sol-gel (TBP-6.12, -6.15, -6.18, -6.26). This is likely due to unavoidable preference and overestimation of affinity by sol-gel assay for the aptamers that were also selected by the same platform.

Unlike the two prior approaches of EMSA and sol-gel, whose analyses are limited to equilibrium properties, a real-time measurement by BLI can be used to study kinetic constants for biomolecular interactions. Such kinetic constants, computed by fitting the first-order rate equation to association and dissociation phase data (Fig. 1(b)), provide an additional insight to biomolecular interactions, and can discriminate aptamers of comparable equilibrium affinity by their difference in kinetic constants to targets. For instance, when the kinetic constants of all seven different aptamers are plotted, most aptamers with higher affinity to TBP were found to possess faster on-rates and slower off-rates (Fig. 1(c)). An

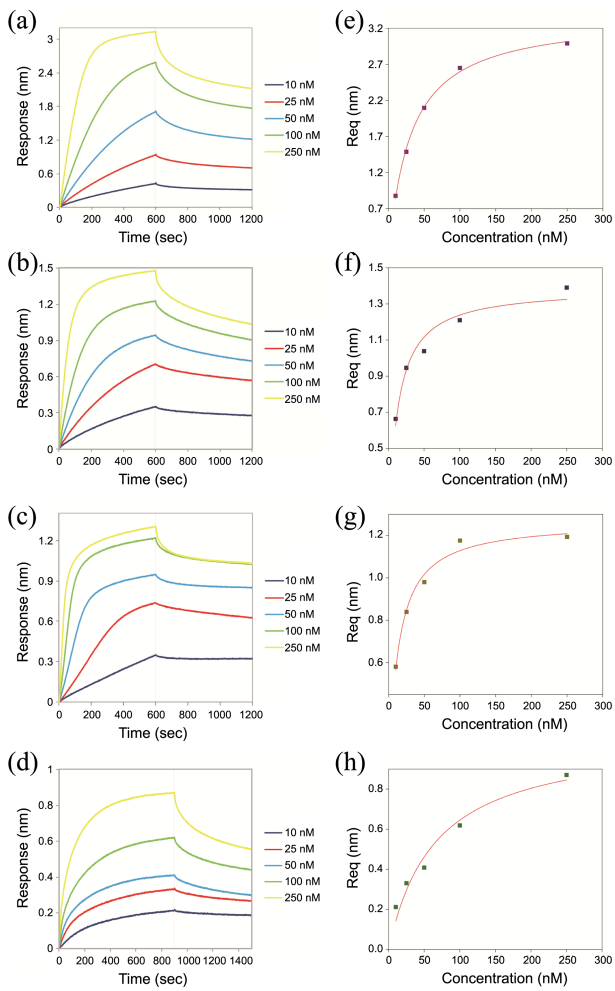

Figure 2. Cross-validation of equilibrium dissociation constants for aptamer and TBP interaction by the kinetic (1:1 rate equation) and the steady-state analyses (Langmuir equation). Shown in the left column are the real-time measurements of the interaction of TBP, used at 10 nM, 25 nM, 50 nM, 100 nM, and 250 nM, with TATA-DNA (a) and TBP-specific aptamers (TBP-6.4, -6.16, and -6.12 for (b), (c), and (d)). On the right column, the steady-state response of the association phase on the left was plotted against the concentration of TBP. The curve-fit of the Langmuir equation to TATA-DNA (e) and aptamer (f-h) binding to TBP is shown in solid line. Equilibrium and kinetics constants, separately predicted from the kinetic and steady-state analyses for aptamer interaction with TBP, are summarized in Supplementary Table 1.

exception to this was TBP-6.12, which bound TBP at 3.4-fold lower affinity compared with TBP-6.4, largely due its faster off-rate. Overall, our data demonstrates that the real-time, multiplexed measurements of aptamer binding to targets by BLI can be used for a rapid discovery of aptamers possessing desired equilibrium and kinetic rates.

Cross-validation of the Binding Constants Estimated by the Kinetic and Steady-state Analyses. The equilibrium dissociation constants (K_D) were obtained separately by fitting the rate equation for 1:1 kinetics (kinetic analysis) and the Langmuir adsorption equation (steady-state analysis) to the data, and were compared for cross-validation (Fig. 2). SA sensors with the aptamers (selected sensorgrams for TBP-6.4, TBP-6.16, and TBP-12 are shown in Fig. 2) were allowed to interact with TBP used at 10-250 nM. Kinetic constants were computed by globally fitting the rate equation to all the data collected at different concentrations. To compute the dissociation constants from the Langmuir equation, the steady-state values were approximated by extrapolating association phase response (corresponding to a phase 'III' in Fig. 1(a)) to saturation. To first show that for a well-defined 1:1 interaction, both methods should yield comparable estimates of K_D, we used a pair of TATA-DNA and TBP for a model interaction (Fig. 2(a) & (e)). The kinetic and steady-state analyses predicted K_D to be 19.1 nM and 30 nM, respectively, differing by ~50% from each other. Overall, the equilibrium constants estimated by either method were close, with an increasing discrepancy observed for lower affinity aptamers (*e.g.*, TBP-6.12, TBP-6.15, TBP-6.18, and TBP-6.26 as shown in Supplementary Table 1). We also noted that the K_D values predicted by the kinetic analysis were consistently lower (higher affinity) (Supplementary Table 1). Several factors would account for this discrepancy, including imperfect curve-fit, the occurrence of conformational change of aptamers after binding to target, and a heterogenous mode of binding.

Real-time Monitoring of the Transcription Factor Pre-initiation Complex (PIC) Assembly. When a saddle-shaped TBP binds to TATA-box DNA element, TBP bends and unwinds DNA, a complex subsequently stabilized by TFIIA binding.[19] Prior to examining aptamer epitopes and specific inhibition of the PIC assembly by aptamers, we tested first if a sequential assembly of TATA-DNA, TBP, and TFIIA can be discerned by BLI. SA biosensors were first incubated with biotinylated TATA-DNA (Fig. 3(a) 'I'), which bound SA tightly with little dissociation occurred after a washing step ('II'). Next, TATA-DNA coated sensors were incubated with TBP ('III') and transferred to washing wells ('IV'), and then to wells containing 0-400 nM of TFIIA (Fig. 3(a) 'V'). Finally, the sensors were transferred to washing wells ('VI') to record the dissociation of TBP/TFIIA from TATA-DNA. Despite the gradual dissociation of TBP from TATA-DNA, TFIIA binding to TBP/TATA complex was clearly discerned by a dose-dependent increase in signals (Fig. 3(a) 'V'). Contrary to a possible role of TFIIA on strengthening TBP and TATA interaction, the stabilizing effect of TFIIA on TBP/TATA complex appeared to be transient, evidenced by

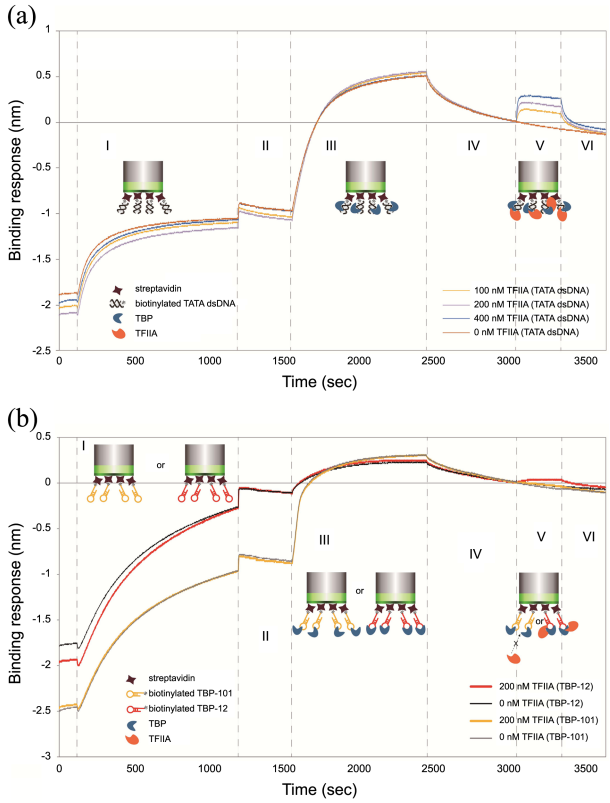

Figure 3. Real-time monitoring of the assembly of PIC and its specific inhibition by TBP aptamers. Real-time sensorgrams using the Bio-layer Interferometer (OCTET RED 384) to study transcription pre-initiation assembly: (a) A series of SA sensors were loaded with 200 nM biotinylated-TATA-DNA (I), washed (II), and were transferred to wells containing 100 nM TBP (III). The sensors were transferred to assay buffer to monitor a dissociation of TBP from TATA-DNA (IV) and then to TFIIA containing wells (V). Subsequently, the dissociation of TBP/TFIIA from TATA-DNA was recorded (VI). (b) TBP aptamers with their epitopes localized to TATA-DNA (TBP-12) or TFIIA (TBP-101) binding sites were attached to SA sensors to recruit TBP, which were then used to probe inhibition of TFIIA binding to TBP.

a rapid reduction of the signals to trace the apparent dissociation kinetics of TBP and TATA-DNA (Fig. 3(a) 'VI').

It has been shown that TFIIA binding to TBP requires prior association of TBP with TATA-DNA.[19] This was also corroborated in our assay, demonstrating that TFIIA binding to TBP captured by even non-competing aptamer (TBP-12) was much lower than to TBP/TATA-DNA complex (Fig. 3(b) 'V' *vs*. Fig. 3(a) 'V'). Consistent with a prior study determining the epitope for TBP-101 to be at TFIIA site, TBP captured by TBP-101 failed to bind TFIIA (Fig. 3(b)).[2]

Epitope Mapping of anti-TBP Aptamers by BLI. Available aptamers against TBP can be categorized into two groups by their recognition of two distinct epitopes, *i.e.*, TATA or TFIIA binding sites. To demonstrate that BLI can be used for a real-time validation of aptamer epitopes, we prepared SA sensors assembled sequentially with TATA-DNA and TBP.[2,3] While TBP-101, whose epitope is at the TFIIA binding site in TBP, formed a ternary complex with

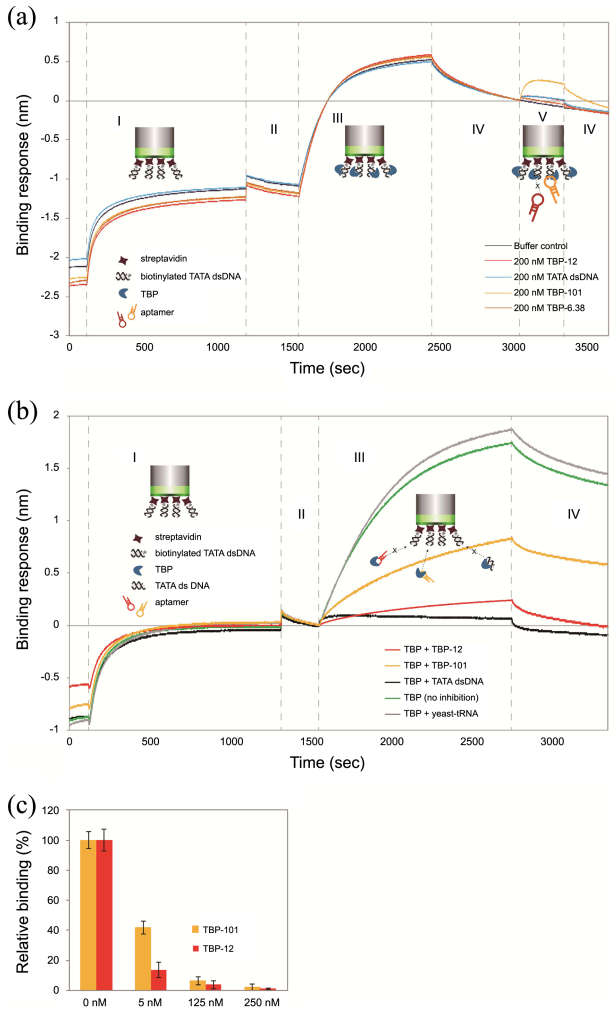

Figure 4. Revealing two classes of TBP aptamers defined by two distinct epitopes in TBP. (a) SA biosensors were assembled with TATA-DNA followed by TBP, and were used to determine aptamer epitopes in TBP. (b) Monitoring specific inhibition of TBP interaction with TATA-DNA by anti-TBP aptamers, irrelevant yeast-tRNA (negative control), and TATA-DNA (positive control). (c) Shown in bar graph is the amount of TBP binding to TATA-DNA and its reduction by TBP aptamers, whose epitopes are at TATA (TBP-12) or TFIIA (TBP-101) binding sites in TBP.

TBP/TATA, little increase was observed with TATA-site specific aptamers, TBP-12 and TBP-6.38 (Fig. 4(a) 'V'). Inhibition of TBP binding to TATA-DNA by anti-TBP aptamers was also monitored by BLI (Fig. 4(b) & (c)). The TATA-DNA loaded SA sensors were incubated with TBP, which was premixed with anti-TATA site aptamer (TBP-12), anti-TFIIA site aptamer (TBP-101), excess TATA-dsDNA (positive control for inhibition), and yeast-tRNA (control for non-specific inhibition). As anticipated, the inhibition of TBP binding to TATA-DNA was higher with TBP-12 by its direct competition with TATA-DNA for binding to TBP (Fig. 4(b)). Interestingly, although TBP-101 recognizes the TFIIA binding site in TBP, it still partially inhibited TBP binding to TATA-box, likely due to the non-specific binding to TATA binding site or the TBP-101 induced conformational change of TBP, making TBP less competent in binding to TATA-DNA. This resulted in, at high concentrations of both aptamers of TBP-101 and TBP-12, inhibition of TBP binding to TATA-DNA (Fig. 4(c)).

Conclusion

The assembly of TBP and other transcriptional complex with RNA polymerase is central to transcriptional activation of a large set of genes in eukaryotes. RNA aptamers have emerged as an important and possibly a unique tool for reversibly and dynamically altering this assembly process with a finer control over specificity. Although the advent of high throughput sequencing technology has greatly facilitated the process of aptamer discovery, the bottleneck to the wider use of aptamers, however, still remains for the lack of quantitative, multiplexed methods for evaluating aptamers as currently available assays are unsuitable for rapidly testing many candidate aptamers with adequate accuracy. Similarly to the great use of surface plasmon resonance for studying biomolecular interactions, here we report that BLI is a powerful platform for achieving label-free, multiplexed detection of biomolecular interactions involving aptamers. Real-time recording of aptamer interaction with targets not only provided equilibrium properties but also kinetic constants, which can discriminate aptamers with comparable affinities to targets. Furthermore, the assembly process of a subset of transcription initiation complex could be monitored by BLI, which was then used to examine aptamer epitopes and specific inhibition of the assembly process.

Acknowledgments. This research was supported by Korea Ministry of Environment as "EI project" (ERL E211-41003-0007-0), and Agency for Defense Development through Chemical and Biological Defense Research Center (2012-0126-005). Global Research Laboratory program by Ministry of Education and Science and Technology in Korea (grant 2008-00582) to D.-K.L supported this work. The Seoul R&BD Program (PA130117) supported this work.

References

1. Roeder, R. G. *Trends Biochem. Sci.* **1996**, *21*, 327.
2. Shi, H.; Fan, X. C.; Sevilimedu, A.; Lis, J. T. *Proc. Natl. Acad. Sci. USA* **2007**, *104*, 3742.
3. Fan, X. C.; Shi, H.; Adelman, K.; Lis, J. T. *Proc. Natl. Acad. Sci. USA* **2004**, *101*, 6934.
4. Sevilimedu, A.; Shi, H.; Lis, J. T. *Nucleic Acids Res.* **2008**, *36*, 3118.
5. Ahn, J. Y.; Jo, M.; Dua, P.; Lee, D. K.; Kim, S. *Oligonucleotides* **2011**, *21*, 93.
6. Wurster, S. E.; Maher, L. J. *RNA* **2008**, *14*, 1037.
7. Zhao, X.; Shi, H.; Sevilimedu, A.; Liachko, N.; Nelson, H. C. M.; Lis, J. T. *Nucleic Acids Res.* **2006**, *34*, 3755.
8. Tuerk, C.; Gold, L. *Science* **1990**, *249*, 505.
9. Kim, S.; Shi, H.; Lee, D.; Lis, J. T. *Nucleic Acids Res.* **2003**, *31*, 1955.
10. Schütze, T.; Wilhelm, B.; Greiner, N.; Braun, H.; Peter, F.; Mörl, M.; Erdmann, V. A.; Lehrach, H.; Konthur, Z.; Menger, M.; Arndt, P. F.; Glökler, J. *PLoS ONE* **2011**, *6*, e29604.

11. Zimmermann, B.; Gesell, T.; Chen, D.; Lorenz, C.; Schroeder, R. *PLoS ONE* **2010**, *5*, e9169.
12. Edwards, K.; Baeumner, A. *Anal. Bioanal. Chem.* **2010**, *398*, 2635.
13. Sekiya, S.; Noda, K.; Nishikawa, F.; Yokoyama, T.; Kumar, P. K. R.; Nishikawa, S. *J. Biochem.* **2006**, *139*, 383.
14. Hellman, L. M.; Fried, M. G. *Nat. Protocols* **2007**, *2*, 1849.
15. Concepcion, J.; Witte, K.; Wartchow, C.; Choo, S.; Yao, D.; Persson, H.; Wei, J.; Li, P.; Heidecker, B.; Ma, W.; Varma, R.; Zhao, L.-S.; Perillat, D.; Carricato, G.; Recknor, M.; Du, K.; Ho, H.; Ellis, T.; Gamez, J.; Howes, M.; Phi-Wilson, J.; Lockard, S.; Zuk, R.; Tan, H. *Comb. Chem. High T. Scr.* **2009**, *12*, 791.
16. Shooltz, D. D.; Alberts, G. L.; Triezenberg, S. J. *Protein Expres. Purif.* **2008**, *59*, 297.
17. Liu, Y.; Shen, L. *Langmuir* **2008**, *24*, 11625.
18. Abdiche, Y.; Malashock, D.; Pinkerton, A.; Pons, J. *Anal. Biochem.* **2008**, *377*, 209.
19. Kang, J. J.; Auble, D. T.; Ranish, J. A.; Hahn, S. *Mol. Cell. Biol.* **1995**, *15*, 1234.
20. Ahn, J. Y.; Kim, E.; Kang, J.; Kim, S. *Nucleic Acid Therapeutics* **2011**, *21*, 179.